# Simulation of photodisintegration of $D_2O$ via UNPOLARIZED photons using GEANT4

O. Kosinov

April 6, 2011

**Abstract**

In this paper the results of heavy water photodisintegration via unpolarized bremsstrahlung photons with end-point energy 25 MeV will be described.

## Contents

## 1   Introduction

The main point was to test and implement gamma-nuclear interaction models in GEANT4, and observe photodisintegration effect of $D_2O$. Energy spectra of neutrons and their angular distributions were obtained.

## 2 Procedure and Results

In order to produce the photodisintegration the following model describing hadronic processes for $< gamma >$ was implemented: PhotonInelastic Models: CHIPS: Emin(GeV)=0 Emax(GeV)=3.5 . The CHIPS model stands for Chiral Invariant Phase Spase model. The accuracy of the G4 simulation of the photodisintegration (Fig.2) was compared to experimental data (Fig.1).

$$\gamma + {}^2\mathrm{H}$$

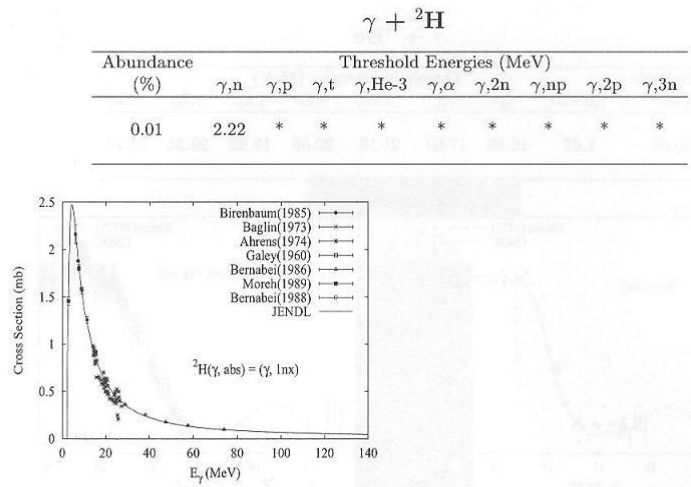| Abundance | Threshold Energies (MeV) | | | | | | | | |
| (%) | $\gamma$,n | $\gamma$,p | $\gamma$,t | $\gamma$,He-3 | $\gamma$,$\alpha$ | $\gamma$,2n | $\gamma$,np | $\gamma$,2p | $\gamma$,3n |
| 0.01 | 2.22 | * | * | * | * | * | * | * | * |



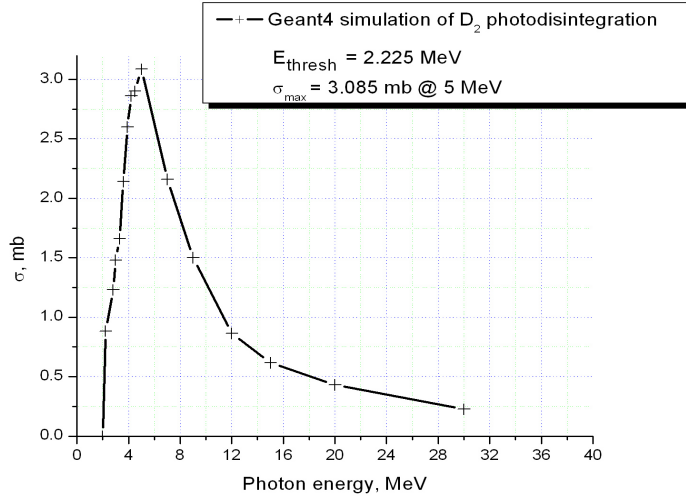Figure 1: Experimental data. Handbook on Photonuclear Data.

Figure 2: G4 simulation.

For verification of the G4 accuracy, the 100% $D_2$ material in a liquid state was used as a target and monoenergetic photons with different energies were thrown on the target. The max value of the experimental photodisintegration cross section is 2.5 mb at 4.48 MeV photon energy. The difference in max values of the experimental and simulated x-sections is 0.585 mb and 0.5 MeV difference for the corresponding energies.

Next, normalized bremmstrahlung spectrum of photons with end-point energy 25 MeV was inserted into G4 (see Fig.3). Then the photons from the spectrum were thrown onto the deuterated water target. The resulting neutron spectrum (see Fig.4) reperesents neutron energies of the neutrons which managed to escape the target and which were produced by different physical processess.
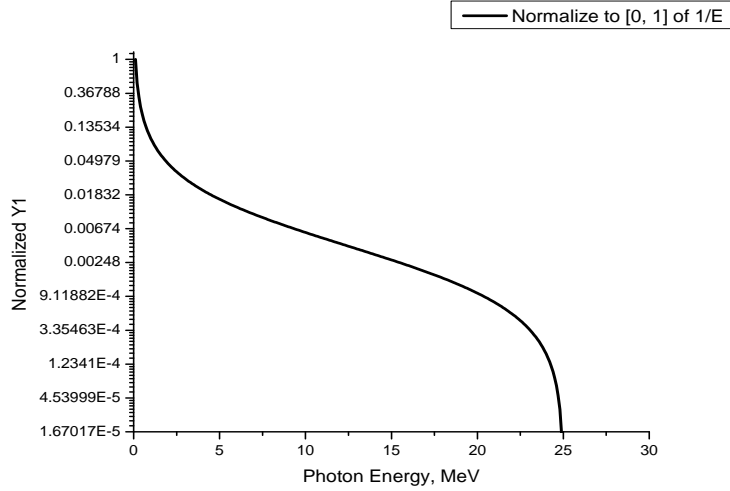
Figure 3: Bremsstrahlung spectrum.

90% enriched $D_2O$ was composed out of the following elements

$$H - 2 = 10.0705\%; H - 1 = 1.1189\%; O - 16 = 88.8106\%; \qquad (1)$$

and its density $1.1056 g/cm^3$. $D_2O$ was shaped into cylinder of 5.5 cm diameter and 18.0 cm hight along the beam line without any shell.

After that it was decided to verify the origin of the neutrons. In order to make the separation of neutron sources more clear, the EM physics for photons was turned off and only gamma-nuclear reactions were active. The correlation plot of energy of the neutrons going out the target and energy of the incident photons is presented in Fig.5. Only secondary neutrons which arose in the primary interaction of the photons with the target material were taken into account.
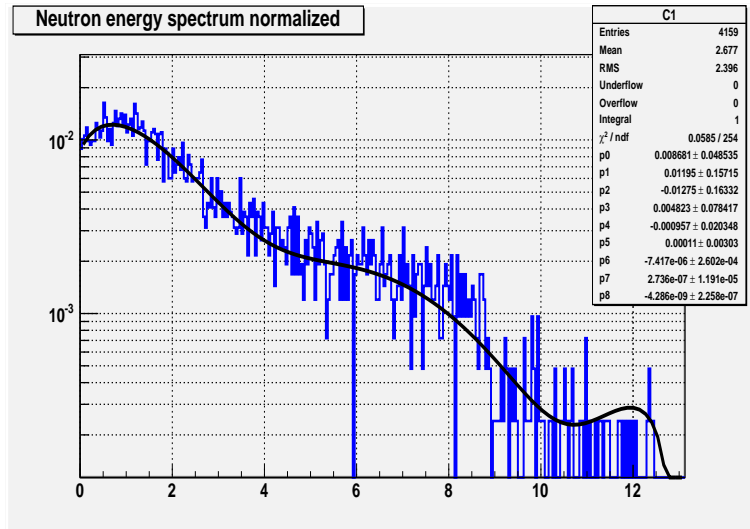
Figure 4: The energy spectrum of neutrons produced by 25 MeV end-point bremsstrahlung spectrum in $90\% D_2O$. EM physics for photons is off.
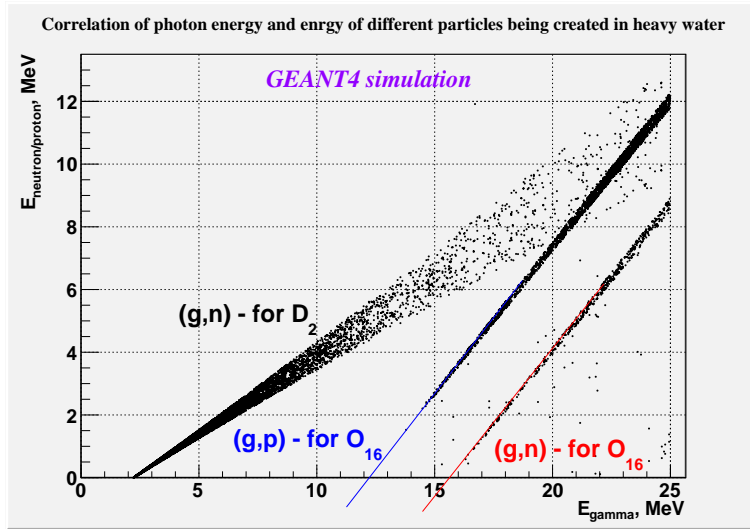


Figure 5: Correlation plot of neutron and proton energies and incident photon energy. $90\% D_2O$ was used as a target. EM for photons turned off. See Fig.6 for threshold values.

5

$$\gamma + {}^{16}\text{O}$$

| Abundance | Threshold Energies (MeV) | | | | | | | | |
|---|---|---|---|---|---|---|---|---|---|
| (%) | $\gamma$,n | $\gamma$,p | $\gamma$,t | $\gamma$,He-3 | $\gamma,\alpha$ | $\gamma$,2n | $\gamma$,np | $\gamma$,2p | $\gamma$,3n |
| 99.76 | 15.66 | 12.13 | 25.03 | 22.79 | 7.16 | 28.89 | 22.96 | 22.34 | 52.06 |

Figure 6: The threshold of neutron photoproduction on O-16. Handbook on Photonuclear Data.

As can be seen from Figs. 1, 5 and 6 the neutrons and protons are produced in photodisintegration of deuterium and in the ($\gamma$,n) and ($\gamma$,p) reactions on oxygen-16. The neutrons originating from oxygen have different energies because the kinematics of the process is different from the one of deuteron photodisintegration.
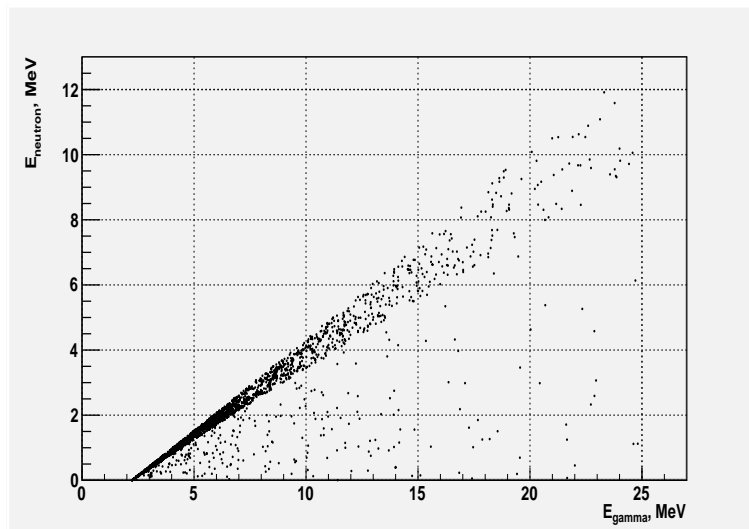


Figure 7: Correlation plot of neutron energy and incident photon energy. EM for photons turned on. 100% solid $D_2$ material.

In Fig.7 the correlation plot is presented for 100% deuterium and there are no events corresponding to ($\gamma$,n) reaction on oxygen. EM interactions of

6

photons with the target material can be observed thruogh the appearence of neutrons with lower energies in the spectrum.
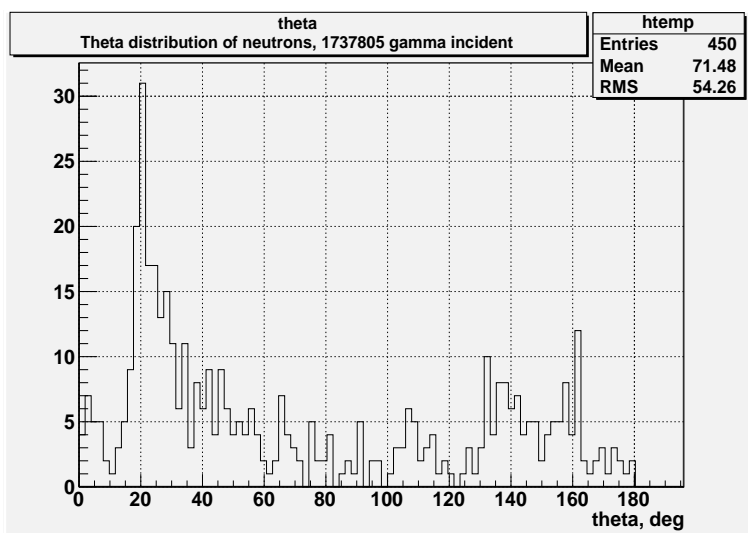
# 3 Neutron angular distributions



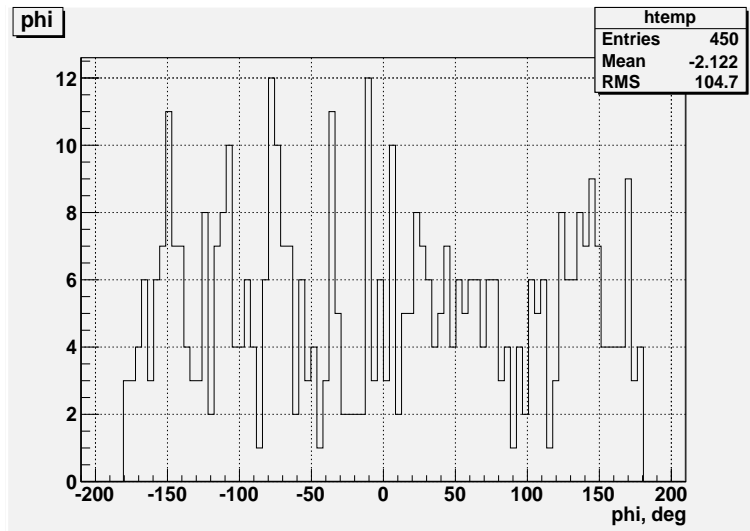Figure 8: Theta distribution of neutrons produced in $90\% D_2O$.

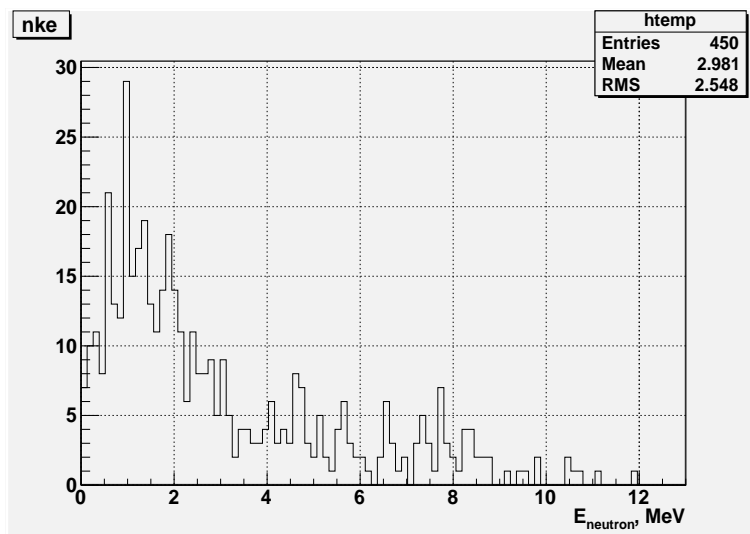Figure 9: Phi distribution of neutrons produced in $90\%D_2O$.



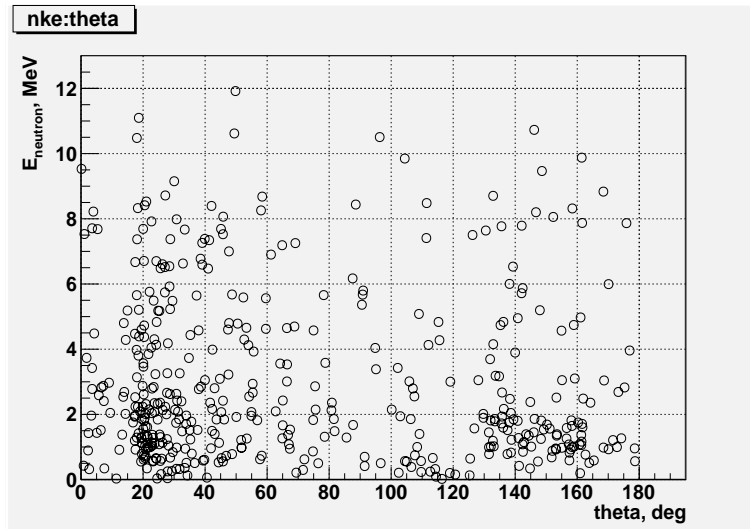Figure 10: Energy distribution of neutrons produced in $90\%D_2O$. EM physics is on for photons.

Figure 11: Correlation of energy distribution of neutrons produced in $90\% D_2O$ and theta angle of emission. EM physics is on for photons.
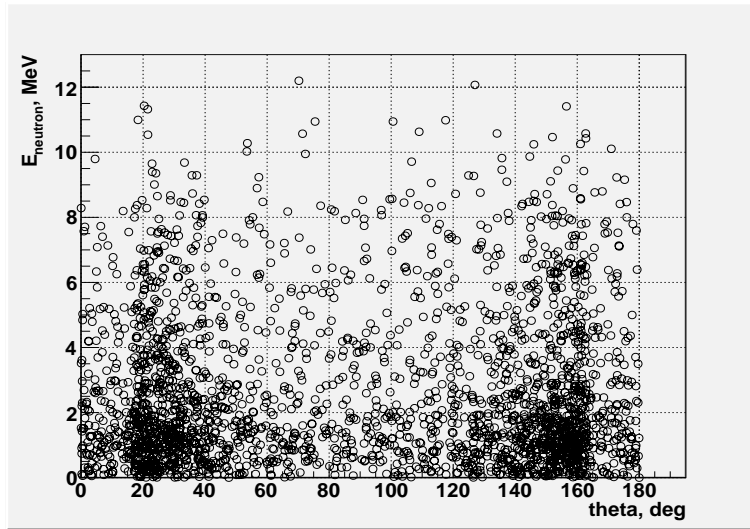


Figure 12: Correlation of energy distribution of neutrons produced in $90\% D_2O$ and theta angle of emission. EM physics is off for photons to reduce the time of simulation.

# 4    TOF simulation

Using neutron energy spectrum shown in Fig. 4 the time-of-flight was re-constructed for the case where neutrons are emitted from the volume of the target. The distance from the target to the detector was varied according to the reaction vertex position. The geometry was inherited from the experiment. Vacuum and $90\%D_2O$ were placed inside the target.

TOF spectrum for the target filled with vacuum is shown in Fig.13. $10^7$ events were sampled and neutrons were detected by our 100% efficient detector.
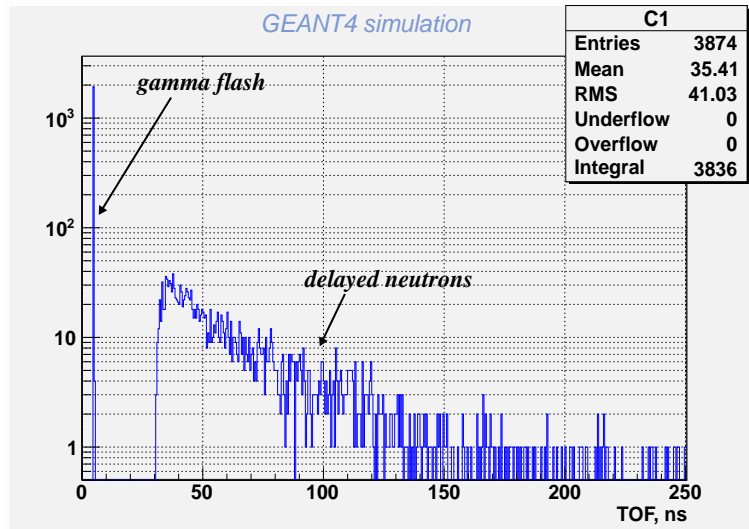


Figure 13:    TOF spectrum of neutrons in the case of volume source filled with vacuum and corresponding to the neutron energy spectrum shown in Fig.4. Zero is the time when the photon hits the target.
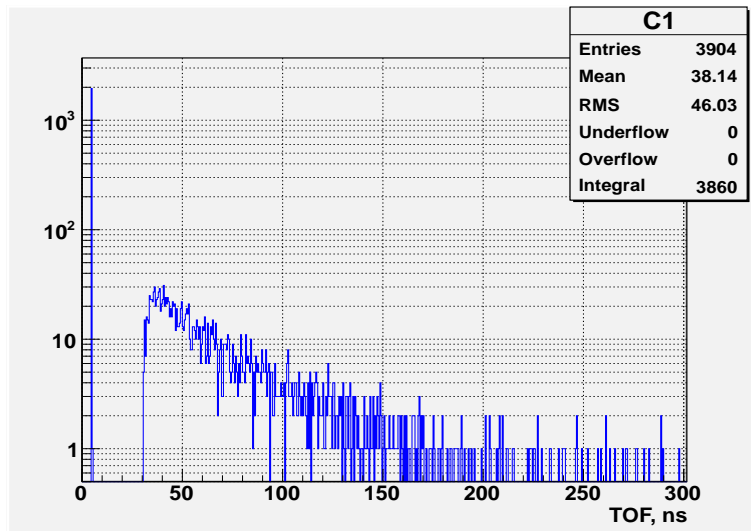
Figure 14: TOF spectrum of neutrons in the case of volume source filled with $90\% D_2O$ and corresponding to the neutron energy spectrum shown in Fig.4. 25 ns gap in between the gammas and neutron region.
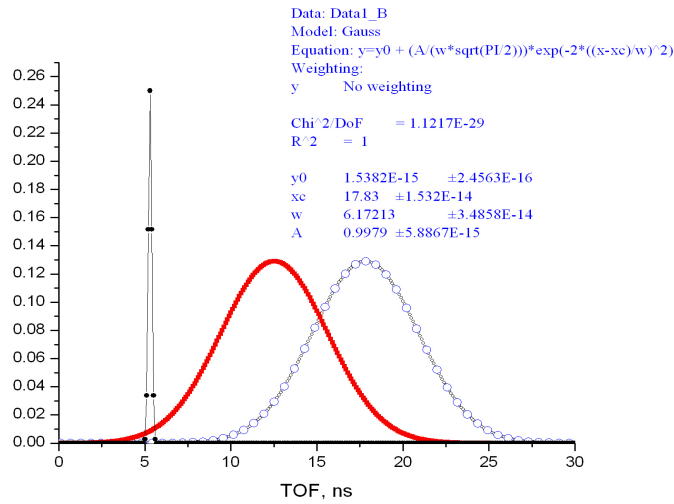
Figure 15: Convolution of beam pulse time distribution and TOF distribution of photons originated in the target. Red curve represents the intensity of photons over the time.
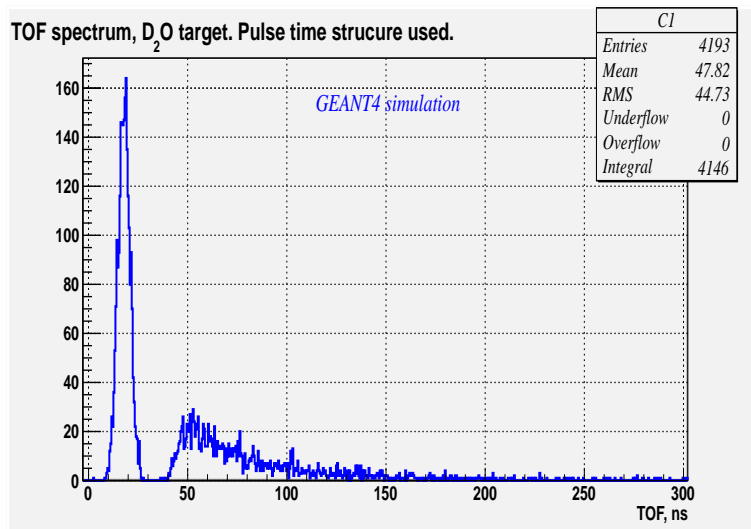


Figure 16: Final TOF spectrum. Start is at $t = 0$. Incident photons have time distribution shown in Fig.15 (red curve).
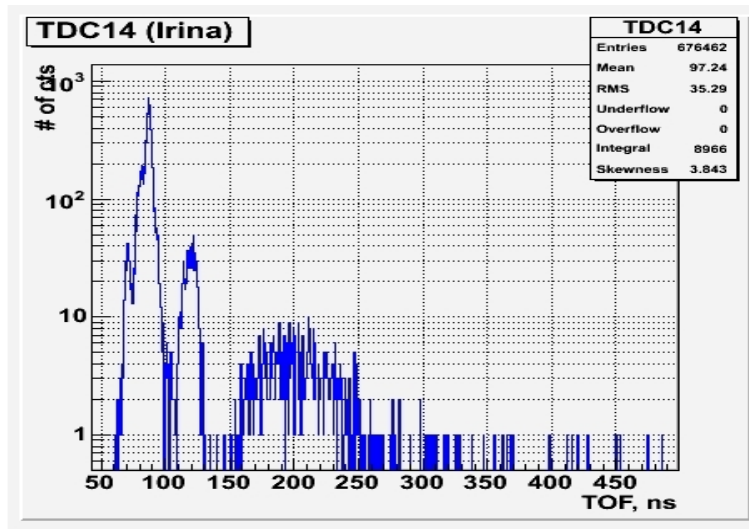
Figure 17: TOF spectrum of neutrons from $D_2O$. Run 1945. Zero is at 85 ns supposedly. 80 ns gap in between photons and neutrons.
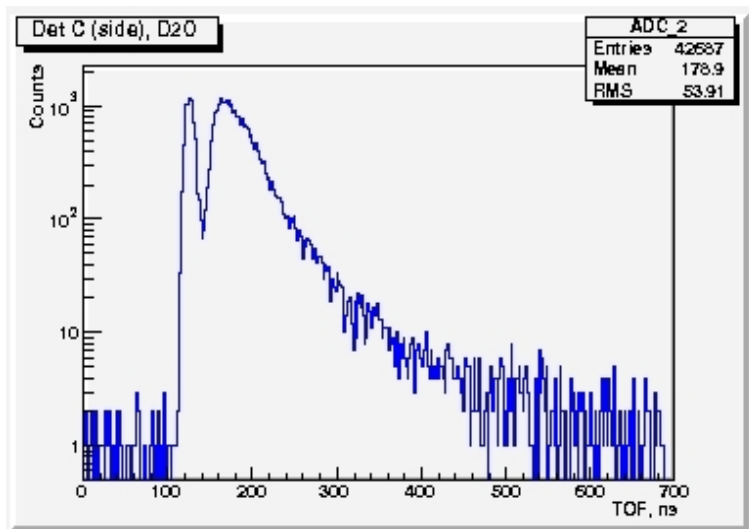


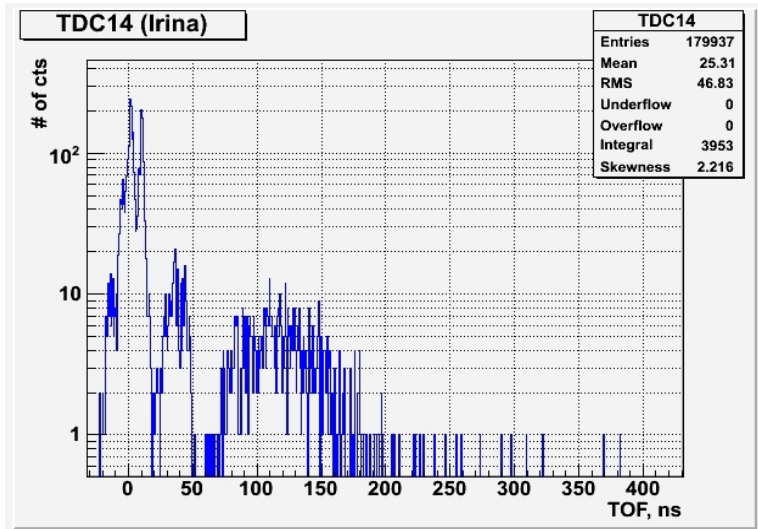Figure 18: TOF spectrum of neutrons from $D_2O$. End-point energy of bremsstrahlung is 14.0 MeV. HRRL.

13

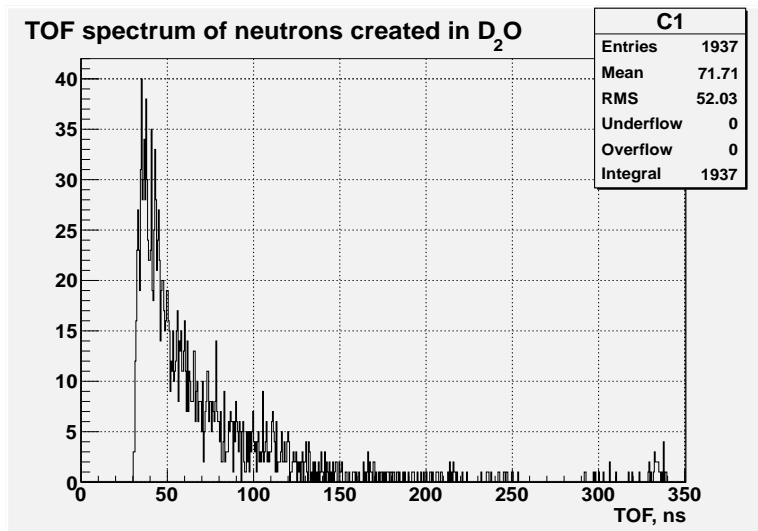Figure 19: Experimental TOF spectrum of neutrons. DU target. Run 1949.



Figure 20: TOF spectrum of neutrons alone.

14

# 5   Separation of neutrons O16($\gamma$,n)O15 from $D_2(\gamma$,n)p

An attempt was made to separate the neutrons being created in two different photo reactions in heavy water. First, two targets having same size and filled with pure $D_2$ and pure O16 were separately irradiated with $10^7$ bremsstrahlung photons (see Fig. 3 for the photon energy spectrum). The data simulated are presented in Fig.21.
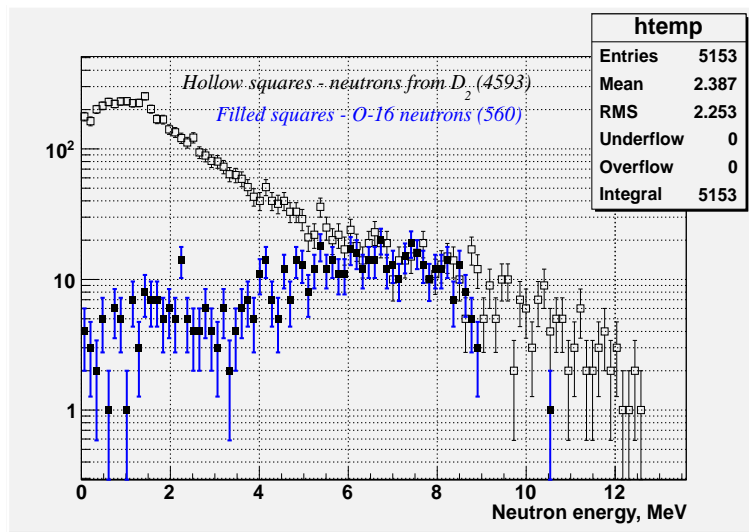


Figure 21:   Neutron energy spectra separation. $4\pi$ yield.

# 6   Results of kinematical constraints

Correlation of neutron energies and incident photon energies was simulated. Using the fact that azimuthal distribution of neutrons created in $D_2O$ in photodisintegration reaction via unpolarized photons is isotropic (see Fig. 9), the uniform ring subtanding the same $\theta$-region as the single detector did was used to detect the neutrons. The results are presented in Figs. 22 and 24. The total number of gammas thrown on the target was $3 \cdot 10^7$
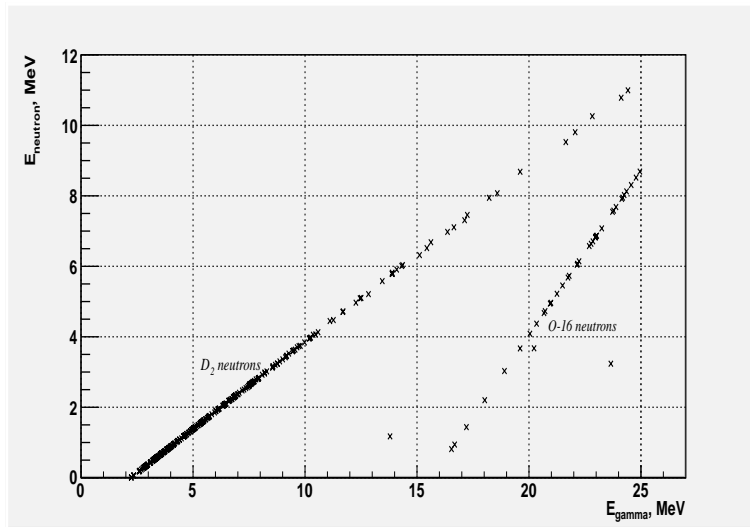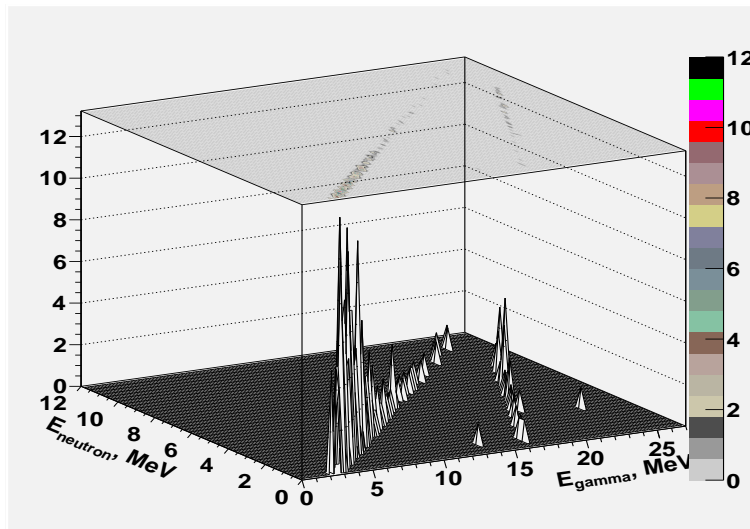
Figure 22:   Correlation plot.
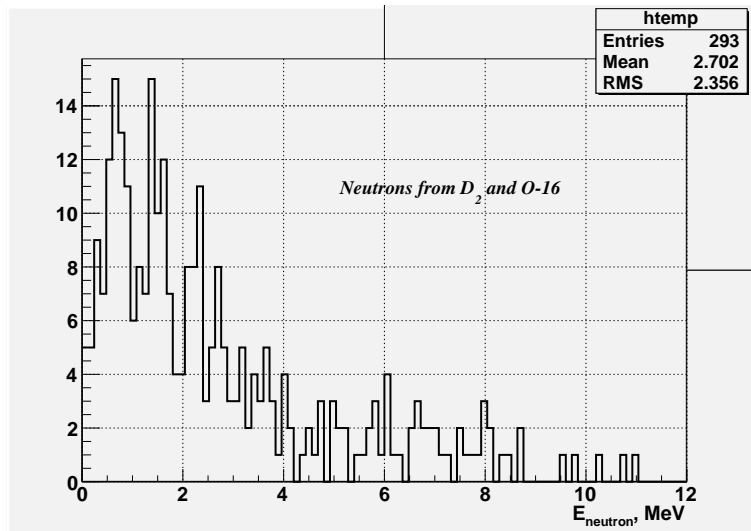


Figure 23:   Correlation plot (surface).

16

Figure 24: Neutron energy spectrum is the sum of neutrons from $D_2$ and $O-16$.

The geometrical efficiency of the detector that has dimensions of scintillating crystall used in the experiment was found to be 0.02%.